Gravitational effect in neutron diffraction by a curved quartz single crystal

V. L. Alekseev, E. G. Lapin, E. K. Leushkin, V. L. Rumyantsev, O. I. Sumbaev, and V. V. Fedorov

B. P. Konstantinov Leningrad Institute of Nuclear Physics, Academy of Sciences of the USSR

(Submitted 28 January 1988)
Zh. Eksp. Teor. Fiz. **94**, 371–383 (August 1988)

An effect of the earth's gravitational field on the diffraction of thermal neutrons in an elastically curved quartz single crystal has been observed experimentally: As the crystal is bent, the contrast of the pendulum pattern decreases more rapidly if the apparatus is oriented in such a way that the effective force due to gravity adds with the Kato elastic force. A theoretical description of the effect is offered.

INTRODUCTION

In Bragg diffraction by a crystal, there is a well-known and unusual amplification effect (see the review by Batterman and Cole,[1] for example): Small changes (within the Bragg width $\Delta\theta_B$) in the angle between the wave vector $\mathbf{k}_0$ of the incident radiation and the system of reflecting planes (i.e., the planes which are near the orientation satisfying the Bragg condition $\lambda = 2d \sin\theta_B$) alter the propagation directions of the rays (Bloch waves) in the crystal over a range much greater than the angle $2\theta_B$. The gain involved here, η, can reach 10^5–10^6:

$$\eta = \frac{\pi}{2}\frac{V}{Fd^2}. \qquad (1)$$

Here V is the volume of a unit cell of the crystal, F is the structure factor of the reflecting planes, and d is the distance between these planes. More specifically, in the case which we will be discussing below, that of the diffraction of thermal neutrons ($\lambda \approx 2\cdot 10^{-8}$ cm) by the $10\bar{1}0$ planes of α-quartz ($F = 8.05\cdot 10^{-13}$ cm, $V = 112\cdot 10^{-24}$ cm^3, $d = 4.255\cdot 10^{-8}$ cm, $\Delta\theta_B \approx 0.8''$), we have $\eta \approx 1.2\cdot 10^5$. For particles which have a charge of some sort (in the case of neutrons, this would be a gravitating mass, a magnetic dipole moment, and possibly an electric dipole moment) it would be extremely tempting to make use of this amplification to study the interaction of the particles with corresponding fields.

There is also the substantial possibility that an interaction will occur directly during the diffraction process, i.e., in the stage of Bloch waves in the crystal, where the field may be very strong. For example, let us consider the diffraction which occurs in a crystal of α-quartz, whose symmetry group does not contain the inversion operation. The positions of the maxima of the neutron density distribution in the crystal are determined primarily by a nuclear interaction. If the reflecting planes are chosen appropriately, these maxima can be put in regions affected by very strong electric fields $\langle\psi|E|\psi\rangle$, ranging up to 3×10^8 V/cm, i.e., ranging up to values some 10^4 times the fields attainable in the laboratory. These fields would correspondingly amplify the effects in a search for an electric dipole moment of the neutron.[2]

One can add to the possibilities here by introducing the elastic curvature of the crystal and thereby changing the symmetry of the problem. For example, a new vector—the so-called Kato elastic force[3]—will arise. By varying the direction (sign) of this force with respect to the force under study, one can in principle obtain a new measurable quantity.

In undertaking work in this direction we decided to begin with the gravitational interaction, in particular, by building on the work begun in Ref. 4.

1. STATEMENT OF THE PROBLEM

We consider a plane-parallel plate; (a rectangular parallelepiped; Fig. 1) which has been cut from a high-quality single crystal of optical α-quartz in such a way that the *hkl* crystallographic planes, whose diffraction is to be used, are normal to the large faces and parallel to the lateral faces. The *hkl* planes are slightly deformed (curved) by an elastic curvature of the plate (in our case, by forces which are concentrated along the "knives" **p** and **p**′). A horizontal beam of unpolarized thermal neutrons is incident on the crystal. The Bragg condition is satisfied for neutrons with a wavelength near 2 Å. Rays (Bloch waves) corresponding to two modes (α and β) propagate in the crystal. These two modes span a certain area $S_{\alpha\beta}$ and form direct and reflected diffracted beams at the exit from the crystal. The measurable beam intensity (the measurements are made by detector D) undergoes oscillations as the crystal is rotated with respect to the incident beam (the angle $\theta_B \propto \lambda$ is changed): One observes a so-called pendulum pattern.

We need to describe the changes which occur in the pendulum pattern as the apparatus *as a whole* is rotated around an axis which coincides with $\mathbf{k}_0$, i.e., as a relative change (a reversal) is made in the direction of the vector **g**, the acceleration due to gravity. A similar problem for a planar (undeformed) crystal was analyzed and solved in Ref. 5. We need to generalize that solution to the case of a deformed crystal.

The magnitude of the deformation required in the reflecting planes of the crystal is set by the curvature of the orbit of neutrons in a gravitational field with a radius of curvature R_n on the order of 1/16 of the earth's radius, i.e., 400 km. At such small deformations, the diffraction by the crystal can clearly be described in the so-called eikonal Kato approximation.[3] In practice, however, it is more convenient to use a slightly different formulation of the eikonal approximation, as set forth in Ref. 6, among other places. We introduce a parameter

$$\alpha = (h^2 + 2(\mathbf{k}_0\mathbf{h}))/k_0^2, \qquad (2)$$

which characterizes the deviation from the Bragg condition (**h** here is the reciprocal-lattice vector of the *hkl* planes of interest, and $\mathbf{k}_0$ is the wave vector of the incident radiation). In a deformed crystal, the reciprocal-lattice vector is some

 0038-5646/88/081727-07$04.00

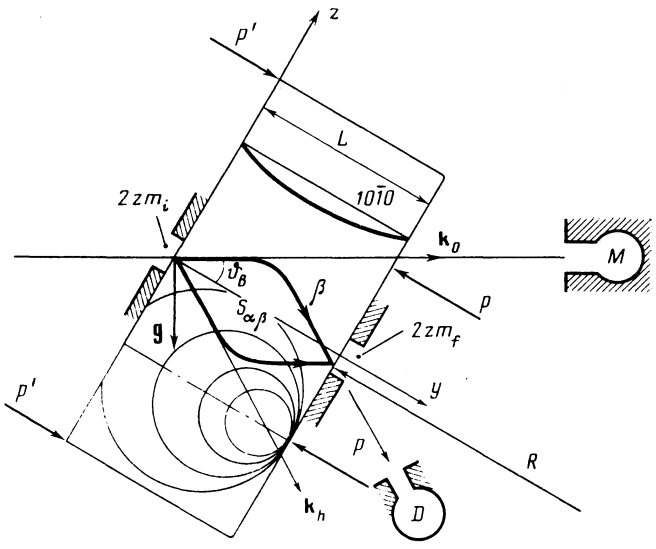

FIG. 1. Schematic diagram of the experiment.

function of the coordinates, $\mathbf{h}=\mathbf{h}(\mathbf{r})$. In our case, the wave vector $\mathbf{k}_0=\mathbf{k}_0(\mathbf{r})$, which rotates and changes in modulus as the gravitational field acts on the neutrons, is also a function of the coordinates. The deformations $\Delta\mathbf{h}=\mathbf{h}(0)-\mathbf{h}(\mathbf{r})$ and $\Delta\mathbf{k}_0=\mathbf{k}_0(0)-\mathbf{k}_0(\mathbf{r})$ are small, so we can ignore $(\Delta\mathbf{h})^2$, $(\Delta\mathbf{k}_0)^2$, $\Delta\mathbf{h}\Delta\mathbf{k}_0$, i.e., α is a linear function of the deformations. In principle, the known relations[6] for the effective Kato force, for the paths traced out by rays in the crystal, and for the phase acquired by the reflected beam at the exit from the crystal furnish the solution of our problem,[1)] in a generalized treatment of the parameter $\alpha(\mathbf{r})$:

$$f(y,z)=-\frac{\pi k_0}{2\cos\theta_B}\left(\frac{\partial}{\partial z}+\frac{1}{c}\frac{\partial}{\partial y}\right)\alpha(y,z), \tag{3}$$

$$\mp\frac{m_0}{c}\frac{d^2z}{dy^2}=f(y,z), \tag{4}$$

$$\varphi(A,B)=\pm m_0 c\int_0^L\left[1-\left(\frac{1}{c}\frac{dz}{dy}\right)^2\right]^{1/2}dy + \frac{\pi k_0}{2\cos\theta_B}\int_0^L\left(1-\frac{1}{c}\frac{dz}{dy}\right)\alpha(y,z)\,dy. \tag{5}$$

Here y and z are the ordinary (dimensional) coordinates (Fig. 1); $c=\tan\theta_B$; $m_0=2Fd/V$ is the effective Kato mass [see (1) regarding the parameters F, d, and V]; L is the thickness of the crystal; A and B are the initial and final points of a path, at the entrance and exit faces; the upper signs refer to the α mode; and the lower signs refer to the β mode.

2. ELASTIC DEFORMATIONS AND KATO FORCES

The forces $\mathbf{pp}'$ (Fig. 1) create a constant bending moment

$$M=pbl, \tag{6}$$

(constant in the region between the inner knives pp), where b is the width of the plate, and l is the distance between neighboring vectors $\mathbf{p}$ and $\mathbf{p}'$. The plate is bent cylindrically to a radius of curvature[7]

$$R=I/Ma_{33}, \tag{7}$$

where $I=bL^3/12$ is the moment of inertia, and a_{33} is the zz component of the elastic-constant tensor. The bending radius of a plate is measured (by means of the deflection Δ of a cylindrically curved reference surface between inner knives pp) with an optical interferometer (Ref. 8, for example). It was necessary, however, to arrange a bending of the reflecting planes in the range estimated above which could be varied and measured in the course of an experiment. This range—radii of curvature on the order of 100 km—lies far beyond the sensitivity of an optical interferometer, as can easily be seen. A solution to this problem was developed on the basis of the circumstance that the normal cross sections in an anisotropic crystal are generally curves, in contrast with those in a isotropic plate. The coefficient which relates the radius of curvature of a cross section (the reflecting planes) to that of the plate,

$$1/R_{hkl}=C/R,$$

however, which is determined by a combination of the components of the elastic-constant tensor a_{ij} (Ref. 9),

$$C=(a_{34}-a_{35}a_{45}/a_{55})/(a_{33}-a_{35}^2/a_{55}), \tag{8}$$

can be made extremely small. It can be varied after the selected crystallographic planes have been brought into coincidence with normal cross sections of the plate, by rotating the cut away from the position corresponding to $R_{hkl}\to\infty$, through a small angle ϕ around the longitudinal axis z, during the fabrication of the plate. In our case we have $\phi=1.5\pm0.1°$ and $C=7.8\cdot10^{-3}$ so we find $R_{hkl}\approx100$ at $R\approx1$ km. The latter values are now amenable to measurement with an optical interferometer.

The limited dimensions (length) of the crystals available (80 mm in our case) lead to limitations on the value of l [29.25 mm in our case; see relation (6)] and thus to fairly large values of the concentrated forces $|\mathbf{p}|=|\mathbf{p}'|$. This circumstance seriously complicates the simple strain pattern which would have prevailed in the case of bending by moments alone:

$$\mathbf{u}=\mathbf{e}_z\frac{CM}{2I}a_{33}\left(y-\frac{L}{2}\right)^2, \tag{9}$$

where $\mathbf{u}$ is the elastic displacement vector, and $\mathbf{e}_z$ is a unit vector along the z axis.

We solved the problem of incorporating the concentrated forces $\mathbf{pp}$ (and $\mathbf{p}'\mathbf{p}'$) in a model of an elastic half-plane which was assumed to be isotropic in the calculation of the stresses. In polar coordinates we have[7]

$$\sigma_r=\frac{2p}{\pi}\frac{\cos\theta}{r},\quad \sigma_\theta=\tau_{r\theta}=0; \tag{10}$$

i.e., the stress contour lines are circles (Fig. 1), and the magnitude of the stress σ_r at the points on a circle are inversely proportional to its diameter. In Cartesian coordinates (y,z) (Fig. 1), we have

$$\sigma_y=-\frac{2p}{\pi}(L-y)^3\left\{\frac{1}{A_+^2}+\frac{1}{A_-^2}\right\},\quad \sigma_z=-\frac{2p}{\pi}(L-y)\cdot\left\{\frac{(a+z)^2}{A_+^2}+\frac{(a-z)^2}{A_-^2}\right\},\quad \tau_{yz}=\frac{2p}{\pi}(L-y)^2\left\{\frac{(a+z)}{A_+^2}-\frac{(a-z)}{A_-^2}\right\}, \tag{11}$$

where

$$A_+=[(L-y)^2+(a+z)^2],\quad A_-=[(L-y)^2+(a-z)^2],$$

and $2a=pp$ (21.5 mm in our case). Using Hooke's law, we find the strains:

$$\begin{aligned}\varepsilon_y&=a_{22}\sigma_y+a_{23}\sigma_z+a_{24}\tau_{yz},\\ \varepsilon_z&=a_{23}\sigma_y+a_{33}\sigma_z+a_{34}\tau_{yz},\\ \gamma_{yz}&=a_{24}\sigma_y+a_{34}\sigma_z+a_{44}\tau_{yz}.\end{aligned}\tag{12}$$

We are now considering a plate which is anisotropic, with coefficients a_{ij} converted from the tabulated values for α-quartz (Ref. 9, for example) to our cut by means of the standard conversion rules. Using relation (3), or the equivalent relation expressed in terms of displacements, the Kato relation (Ref. 3, III, relation 3)

$$f(y,z)=-\frac{2\pi}{d\sin 2\theta_B}\left[\frac{\partial^2 u_z}{\partial y^2}\cos^2\theta_B-\frac{\partial^2 u_z}{\partial z^2}\sin^2\theta_B\right],\tag{13}$$

and the definitions

$$\varepsilon_z=\frac{\partial u_z}{\partial z},\quad \varepsilon_y=\frac{\partial u_y}{\partial y},\quad \gamma_{yz}=\frac{\partial u_z}{\partial y}+\frac{\partial u_y}{\partial z},$$

we find explicit expressions for the Kato forces. Omitting the trivial but laborious calculations, we write the results:

$$f_p=f_{p1}+f_{p2},$$

$$\begin{aligned}f_{p1}(y,z)=-\frac{8p(L-y)}{d\sin 2\theta_B}\Bigg\{&\frac{a+z}{A_+^3}[(a+z)^2A_c-(L-y)^2A_s]\\&-\frac{a-z}{A_-^3}[(a-z)^2A_c-(L-y)^2A_s]\Bigg\},\end{aligned}\tag{14}$$

where

$$\begin{aligned}A_c&=(a_{44}/2)\cos^2\theta_B+a_{33},\\ A_s&=(a_{44}/2)\sin^2\theta_B-a_{23};\end{aligned}$$

$$\bar f_{p1}(z)=\frac{1}{L}\int_0^L f_{p1}(y,z)\,dy\approx-\frac{8pz}{d\sin 2\theta_B}\frac{L(L^2+3a^2)}{a^2(L^2+a^2)^2}a_{22}\cos^2\theta_B,\tag{14'}$$

$$\bar f_{p2}=\frac{1}{L}\int_0^L f_{p2}(y)\,dy\approx-\frac{8p}{d\sin 2\theta_B}\frac{2L^2}{(L^2+a^2)^2}a_{24}\cos^2\theta_B.\tag{15}$$

The moments M themselves give us [see (9)] the Kato force:

$$f_M=-\frac{8p}{d\sin 2\theta_B}\frac{3\pi l}{L^3}Ca_{33}\cos^2\theta_B.\tag{16}$$

Substituting in our numbers, we find (in units of $-8p\cos^2\theta_B/d\sin 2\theta_B=-4p/dc$)

$$\begin{aligned}\bar f_{p1}(z)&=60.4\cdot 10^{-8}z\ \text{kg}^{-1};\quad \bar f_{p2}=1.0\cdot 10^{-8}\ \text{kg}^{-1},\\ f_M&=6.8\cdot 10^{-8}\ \text{kg}^{-1}.\end{aligned}\tag{17}$$

The most important point is the appearance, when the concentrated forces are taken into account, of a variable force $f_{p1}(y,z)$, which depends on the coordinates y and z. The dependence on the coordinate z is essentially linear at the small values ($z/a\ll 1$) typical of our problem. This point is illustrated, in particular, by relation (14'), which was found by averaging (14) over the coordinate y and by retaining the most important terms. The physical origin of this component of the force is understood; put somewhat crudely, the reason is the "overstressing" of the cross sections (the reflecting planes) which reproduces circles of $\sigma_r=\text{const}$ (Fig. 1) under the influence of the concentrated forces. This overhang changes sign halfway between the forces **p**. The component f_{p2} arises only as a result of the anisotropy (in an anisotropic object we would have a coefficient $a_{24}=0$) and is relatively small. We are giving its average value (over y) in (15); it is this average value which we will use below.

The resultant Kato force due to the elastic deformation can be written

$$f=f_0(1+\beta z),\tag{18}$$

where

$$f_0=-\frac{4p}{dc}(f_M+\bar f_{p2})=\text{const},$$

$$\beta(y)=\frac{f_{p1}(y,z)}{z(f_M+\bar f_{p2})},\quad \bar\beta=\frac{\bar f_{p1}(z)}{z(f_M+\bar f_{p2})}=7.8\,\text{cm}^{-1}$$

[see endnote 2)]. Incorporating the concentrated forces **pp** also causes a substantial change in the shape of the reference surface and, correspondingly, a change in the relation between the measured deflection of this surface, Δ, and the concentrated forces $|\mathbf{p}|=|\mathbf{p}'|$ which are to be determined. This new relation can be derived easily for the problem discussed above:

$$\frac{\Delta}{p}=\frac{6la^2}{L^3}a_{33}\left[1+\frac{L^3}{3\pi a^2 l}\left(\ln\frac{L^3}{3\pi a^2 l}-1\right)\right].\tag{19}$$

3. EFFECTIVE FORCE DUE TO GRAVITY; RAY PATHS IN THE CRYSTAL; PHASE DIFFERENCE BETWEEN THE INTERFERING REFLECTED BEAMS; PENDULUM PATTERN

The wave vector $\mathbf{k}_0$ in a gravitational field can be written

$$\mathbf{k}_0(\mathbf{r})=\mathbf{k}_{0g}+\mathbf{k}_g=\mathbf{k}_0\left(1+\frac{m_n^2}{2\pi^2\hbar^2k_0^2}\mathbf{gr}\right)^{1/2}+\frac{m_n^2y}{4\pi^2\hbar^2k_0\cos\theta_B}\mathbf{g}.\tag{20}$$

Here m_n is the mass of a neutron, and $\hbar$ is Planck's constant. The first term in (20) incorporates the change in the modulus of the vector $\mathbf{k}_0$ (the gravitational "reddening" of the neutrons); the second incorporates the change in the direction of $\mathbf{k}_0$ due to the appearance of a neutron velocity component as a result of the acceleration **g**. Expression (2) for $\alpha(y,z)$ can be written as follows in this case:

$$\begin{aligned}\alpha(y,z)=&\frac{h^2}{k_0^2F(y-z/c)}-\frac{2k_0h\sin\theta_B}{k_0^2[F(y-z/c)]^{1/2}}\\&+\frac{2m_n^2gh}{4\pi^2\hbar^2k_0^3}\frac{y}{F(y-z/c)},\end{aligned}\tag{21}$$

where

$$F\left(y-\frac{z}{c}\right)=1+\frac{m_n^2g}{2\pi^2\hbar^2k_0^2}\left(y-\frac{z}{c}\right)\sin\theta_B.$$

The particular geometry in Fig. 1 was taken into account in (21).

Calculating $f_g(y,z)$ from (3), we find that the first two

terms in (21) do not contribute to f_g in our case, since the application of the operator $\partial/\partial z + c^{-1}\partial/\partial y$ to the function $F(y - z/c)$ gives us zero. As a result we find

$$f_g = -\frac{m_n^2 g}{\hbar^2 K} \Big/ \left[1 + 2\frac{m_n^2 g}{\hbar^2 K^2}\left(y - \frac{z}{c}\right)\sin\theta_B \right].$$

Ignoring the term $\sim m_n^2/\hbar^2 K^2 \approx 10^{-8}$ in the denominator, we finally find

$$f_g \approx -m_n^2 g/\hbar^2 K = \text{const}, \tag{22}$$

where $K = 2\pi k_0$. Along with force (18), caused by the elastic deformation, the effective gravitational force f_g (which is constant) forms the complete effective force of our problem:

$$f = f_0(1+\beta z) \pm f_g. \tag{23}$$

The plus sign in front of f_g corresponds to the situation in Fig. 1, in which the bending of the reflecting planes and the rotation of $\mathbf{k}_0$ in the gravitational field cause additive changes in the diffraction angle. The situation after the rotation of the apparatus (which simply amounts to a change in the sign of $\mathbf{g}$ in Fig. 1) corresponds to the minus sign in (23).

The paths $z(y)$ of the α and β rays in the crystal, which are described by the differential equation (4), unfortunately cannot be expressed in quadratures with the complicated functional dependence $\beta(y)$ calculated above. We thus prefer to replace $\beta(y)$ by a value averaged over the crystal thickness. After this replacement is made, Eq. (4) becomes linear with constant coefficients and can be solved quite easily:

$$\frac{d^2 z}{dy^2} = \mp\frac{c}{m_0}[f_0(1+\bar{\beta}z) \pm f_g] \tag{24}$$

or

$$\frac{d^2 z}{dy^2} - A_0^2 z = A_0^2 B_0,$$

where the $\mp$, which correspond to the α and β modes, have been incorporated in m (i.e., we have assumed $m_0 = |m|, m_\alpha < 0, m_\beta > 0$, and where we have introduced

$$A_0^2 = \frac{cf_0}{m}\bar{\beta}, \quad B_0 = \frac{1 \pm f_g/f_0}{\bar{\beta}},$$

$$z_\beta = B_0 \frac{(1+z_f/B_0)\sin(|A_0|y) + (1+z_i/B_0)\sin[|A_0|(L-y)] - \sin(|A_0|L)}{\sin(|A_0|L)} \tag{25}$$

for $A^2 < 0$, i.e., for the β ray in Fig. 1, with $m_\beta > 0, f_0 < 0$; or

$$z_\alpha = B_0 \cdot \frac{(1+z_f/B_0)\,\mathrm{sh}(|A_0|y) + (1+z_i/B_0)\,\mathrm{sh}[|A_0|(L-y)] - \mathrm{sh}(|A_0|L)}{\mathrm{sh}(|A_0|L)}$$

for $A^2 > 0$. Solutions were found under the boundary conditions

$$\begin{aligned} z_\alpha = z_\beta = z_i \quad &\text{at} \quad y = 0, \\ z_\alpha = z_\beta = z_f \quad &\text{at} \quad y = L, \end{aligned} \tag{26}$$

which require a "creation" of the rays at the point z_i at the entrance face and their "annihilation" into diffracted beams at the point z_f at the exit face of the crystal.

Turning to the calculation of the quantity of direct interest here, the phase difference between the interfering reflected beams which have passed through the crystal in the form of the α or β mode,

$$\Delta\varphi_{\alpha\beta} = \varphi_\alpha(A, B) - \varphi_\beta(A, B),$$

we note that the replacement $\beta(y) \to \bar{\beta}$ is equivalent to the introduction of an energy conservation law $T + U = E - \text{const}$ in equation (4), if we think of this equation as an analog of the equation of motion of a particle of mass m/c in a time $y \to t$. In this case, expression (5) for the phase can be rewritten as

$$\varphi(A, B) = S(A, B) = \int_0^L \mathscr{L}\, dy, \tag{27}$$

where

$$\mathscr{L} = -mc + \frac{m}{c}\frac{1}{2}\left(\frac{dz}{dy}\right)^2 - U(z) = -mc + T - U(z)$$

is the Lagrangian, T is the kinetic energy, and U is the potential energy. Since a variation of the action (phase) (5) leads to equations of motion (24) with force (23), the potential energy corresponding to this force in (27),

$$U(z) = (f_0 \pm f_g)z + f_0\bar{\beta}z^2/2,$$

agrees with the potential term in (5) to within an inconsequential second derivative with respect to y.

Using (26), we thus find the following result from the conservation law:

$$\mathscr{L} = -mc + E - 2U(z) = -mc + \frac{m}{2c}\left(\frac{dz}{dy}\right)_L^2 - 2U(z).$$

As a result, allowing for the different signs of the masses m for the α and β modes, we find

$$\Delta\varphi_{\alpha\beta}(z_i, z_f) = 2m_0 cL - \frac{m_0 L}{2c}\left[\left(\frac{dz_\alpha}{dy}\right)_L^2 + \left(\frac{dz_\beta}{dy}\right)_L^2\right] + 2(f_0 \pm f_g)\int_0^L (z_\alpha - z_\beta)\,dy + \bar{\beta}f_0\int_0^L (z_\alpha^2 - z_\beta^2)\,dy. \tag{28}$$

Finally, we can write an explicit expression for a characteristic which can be observed experimentally: the behavior of the intensity of the reflected beam, measured by a detector, as a function of the neutron wavelength λ to which the instrument is tuned. This expression is

$$I(\lambda)=\frac{1}{4z_{im}z_{fm}}\int_{-z_{im}}^{z_{im}}\int_{-z_{fm}}^{z_{fm}}\Big[1+\exp\Big(-\frac{\rho^2}{16\ln 2}\Delta\varphi_{\alpha\beta}{}^2\Big)\cos(\Delta\varphi_{\alpha\beta})\Big]dz_i\,dz_j. \quad (29)$$

In this case the wave function of a neutron is the reflected beam is a superposition of the waves which have passed through the crystal in the form of α and β modes:

$$\Psi_{\alpha,\beta}(x)=C_{\alpha,\beta}\exp\left[-P(x_{0\alpha,\beta}-x)^2\right]\exp\left[i(K_h x+\varphi_{\alpha,\beta})\right] \quad (30)$$

(x is the coordinate along the reflected beam). In other words, it is expressed in terms of wave packets (or trains) of Gaussian shape which are filled with a "carrier" of wave vector $K_h = 2\pi/\lambda$. The difference between the positions of the centers of the trains is $x_{0\alpha} - x_{0\beta} = \Delta\varphi_{\alpha\beta}/K_h$. The parameter P is determined by the total relative width at half-maximum ($\rho = \Delta\lambda_{1/2}/\lambda = 1/280$ in our case) of the spectral "line" selected by the diffractometer. The shape of this "line" is also assumed to be Gaussian:

$$P=\frac{\rho^2}{16\ln 2}K_h^2. \quad (31)$$

The exponential factor in (29) thus reflects the degree of overlap of the interfering trains. The cosine which is determined by $\Delta\varphi_{\alpha\beta}(z_i,z_f)$ describes the pendulum pattern. The integrations incorporate the finite widths of the entrance slit ($2z_{im} = 0.8$ mm) and the exit slit ($2z_{fm} = 0.8$ mm) (Fig. 1).

4. EXPERIMENTAL APPARATUS, PROCEDURE, AND RESULTS

A necessary condition for observing effects of the dynamic theory of diffraction, on which the entire discussion is based, is that the single crystal be of high quality. As a quantitative characteristic of the quality required we can use the condition

$$\omega_g/\Delta\theta_B \ll 1, \quad (32)$$

where ω_g is the "mosaicity" of the crystal: a measure of the width of the diffraction line and the integral reflection coefficient in the well-known model of an ideally mosaic crystal. In practice, the parameter ω_g can be measured in the diffraction of sufficiently hard γ radiation. In our case, a selection of single crystals on the basis of the parameter ω_g was carried out with the help of a γ diffractometer at the γ line at 412 keV (Ref. 10). As a result of these measurements, it was found possible to prepare a plate of the necessary orientation with dimensions of $80\times48\times19.99$ mm, with a ω_g value in the interval 0.1–0.2″ in the central part of the plate. The orientation of the cut was set during the preparation. The final position of the reflecting planes (parallel to the lateral faces of the parallelepiped) and the rotation angle $\phi = 1.5°$, which determines f_M (see the discussion above), were checked on an x-ray diffractometer by the Bragg method. They were found to satisfy the requirements to within an error on the order of an arc minute.

The ends of the crystal (to a depth $l = 29.25$ mm from each side) were squeezed between plane bronze mirrors. A lower pair of mirrors was held fixed. A bending force was applied to an upper pair by means of a lever arm and a micrometer screw. As a result, forces distributed correspondingly along the corners of the mirrors (**p**) and the edges of the plate (**p′**) were applied to the crystal. The exposed concave surface (*pp* in Fig. 1) was used as one of the mirrors of an optical (laser) interferometer. The second mirror was a high-quality plane mirror, which was inclined at a small angle with respect to the generatrix of the cylindrical surface of the crystal which was the object of the measurements (the reference surface). A pattern of interference fringes arises; the fringes reproduce the shape of the reference surface in enlarged scale [see relation (19), for example]. The deflection of the interference fringes δ, measured after photography, makes it possible to determine the unknown deflection Δ:

$$\Delta=\frac{1}{2}\frac{\delta}{H}\lambda_{opt} \quad (33)$$

[H is the distance between neighboring (similar) interference fringes on the photograph, and $\lambda_{opt} = 0.63$ μm is the wavelength of the light from the laser]. From relation (19) we also find the force $|\mathbf{p}| = |\mathbf{p}'|$.

We used a neutron beam from the horizontal channel of a VVR-M reactor, which was formed by a polarizing neutron duct[3] in the channel and a single-slit collimator. On the crystal the beam produced a spot with dimensions of 30 mm (the horizontal dimension) and 0.8 mm. Figure 2 shows some typical experimental curves of the pendulum pattern. The intensity of the reflected beam (the number of counts at detector D in Fig. 1 over 500 s) is plotted along the ordinate axis; plotted along the abscissa axis is the number L of turns of the drive which sets the diffraction angle θ_B, i.e., the wavelength λ (which increases toward the right along the axis) to which the instrument is tuned (1 turn corresponds to 8″, i.e., to a wavelength increment of 0.0192 Å). As the angle θ_B is changed, the detector moves, tracking the angle $2\theta_B$. We recorded and compared curves in the lower posi-

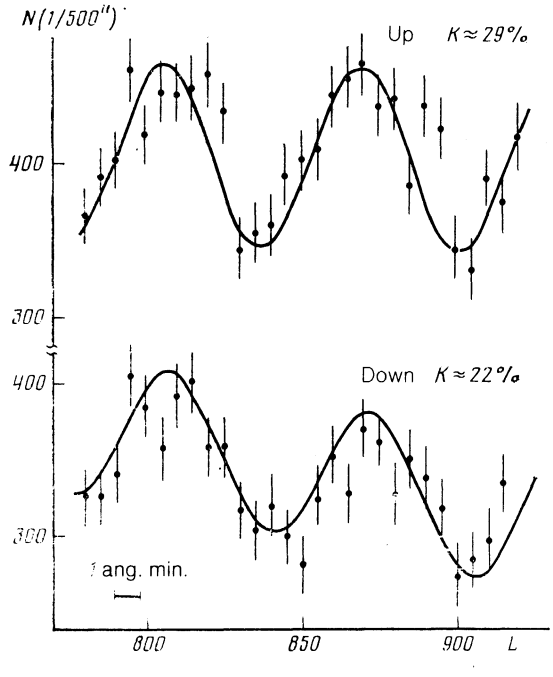

FIG. 2. Examples of the pendulum patterns observed experimentally for the upper and lower positions of the instrument. (The background levels are 200 and 135 counts over 500″, respectively.)

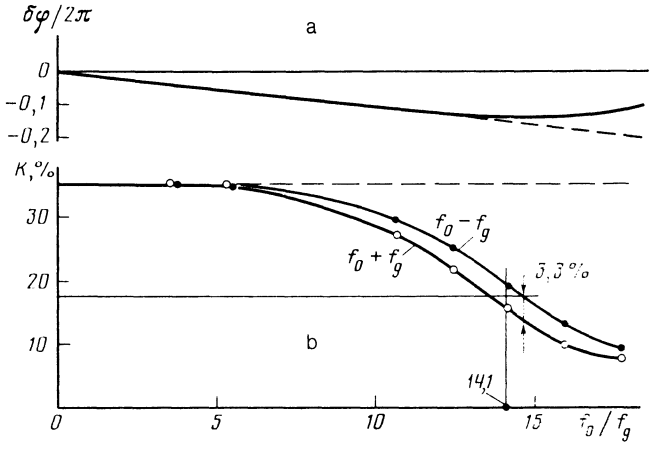

FIG. 3. Theoretical behavior of two quantities as functions of the extent of curvature of the crystal. a—Phase difference between the pendulum cosine waves; b—contrast of the pendulum cosine waves in the lower ($f_0 + f_g$) and upper ($f_0 - f_g$) positions of the instrument.

tion of the instrument (with the detector at the bottom) and in the upper position as the instrument as a whole was rotated 180° around an axis coinciding with the direct beam. The position and intensity of the direct beam were monitored by monitor M. The adjustment which was carried out brought the rotation axis of the instrument into coincidence with the center of gravity of the beam (in the vertical plane) with an error no worse than 0.1 mm. For each pair of pendulum curves corresponding to a given bending of the crystal (the bending was calibrated with the help of an optical interferometer), we found the phase difference

$$\delta\varphi/2\pi = (\lambda_H^* - \lambda_B^*)/\Delta\lambda_T \qquad (34)$$

(λ_H^* and λ_B^* are the positions of the equal-phase points on the pendulum curves for the lower and upper positions of the instruments, respectively; $\Delta\lambda_T$ is the period of the pendulum cosine waves). We also determined the contrast

$$K[\%] = \frac{I_{max} - I_{min}}{I_{max} + I_{min}} \cdot 100, \qquad (35)$$

where $I_{max(min)}$ is the intensity at the maximum (minimum) of the oscillations minus the background, which was determined by displacing the detector from the $2\theta_B$ position. The dashed lines in Fig. 3, a and b, show the results which we initially expected, as calculated from relations of the form (28), (29), (34), and (35)—the ordinates—and (18)—the abscissas. Specifically, we intended to trace the gravitational effect $\delta\varphi/2\pi$, which increases linearly with the curvature of the crystal (with the force f_0) up to values $\delta\varphi/2\pi \approx 1$.

The first experimental results were discouraging: The pendulum pattern, which could reliably be observed on a plane crystal or a crystal curved very slightly, inevitably disappeared (the contrast dropped to zero) as the curvature was increased. The gravitational phase difference $\delta\varphi$ which could barely be detected before (which was nearly within the error) also returned to zero. On the other hand, we noted that as the curvature of the crystal was increased the contrast would disappear first when the instrument was in the lower position (the case $f_0 + f_g$ in the situation in Fig. 1). Figure 2 shows one example of this situation. There was the possibility that this was some unusual manifestation of a gravitational effect.

In a search for an explanation we carried out a more detailed analysis of the conditions prevailing during the curvature of our crystal (Sec. 2), and we examined the role played by the concentrated forces **pp'**. The most important result of this analysis was the observation of a force $f_{p1}(y, z)$ [or $\bar{f}_{p1}(z)$] which depends on the coordinate z—relations (14) and (14') and, correspondingly, a parameter β [see (18)], which we had originally ignored. (The dashed lines in Fig. 3 were calculated for $\beta = 0$). We also varied the calibration of the forces **pp'** through the deflection of the reference surface, i.e., the f_0 scale along the abscissa axis for the experimental data. [During bending by pure moments, the second term in square brackets in (19) is absent.] The results of the calculations for $\bar{\beta} = 7.8\ \text{cm}^{-1}$ [see (18)] are shown by the solid lines in Fig. 3. We recall that although the calculations are approximate, they do not contain any adjustable parameters. Figure 4 summarizes the results of series of experiments. The horizontal error bar on one of the points shows our estimate of the error in the calibration of the experimental abscissa scale in terms of Δ ($\approx \pm 10\%$).

Comparing Figs. 3b and 4, we conclude that the theoretical and experimental curves definitely do agree qualitatively.[4)] At a quantitative level, there is a completely satisfactory agreement ($\approx 10\%$) in terms of the scale along the abscissa axis (the abscissas corresponding to a 50% decrease in the contrast are 14.1 and 12.9, respectively). This agreement is evidence that the description of the reference surface, the force calibration procedure, the calculations, and the overall calibration of the Kato forces are all quite good. The theory correctly reproduces the absolute value and general behavior of the contrast with increasing deformation. As would be expected on the basis of general considerations, the effect vanishes when the crystal is straightened out. However, the gravitational effect—the difference between the contrasts in the positions $f_0 - f_g$ and $f_0 + f_g$—looks slightly larger, on the average, in the experiments (by a factor of 1.8 ± 0.6, where 0.6 is the mean square error of the experimental result) than that predicted by the theory. The mean experimental value found through an approximation by straight lines (the dashed curves in Fig. 4) is $6 \pm 2\%$. The maximum theoretical value is $\Delta K = 3.6\%$. The mean theoretical value, corresponding to the experimental mean value,

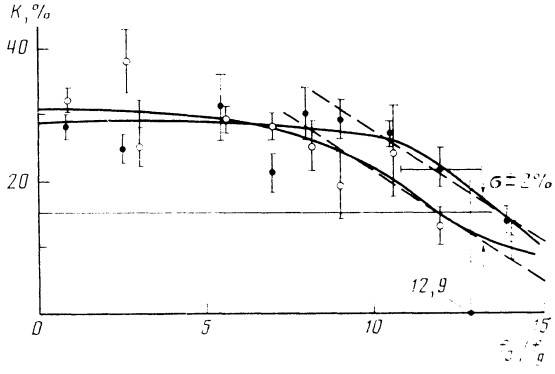

FIG. 4. Experimental results on the contrast of the pendulum patterns versus the curvature of the crystal. ●—Upper position of the instrument; ○—lower position. The distance between arrows corresponds to $6 \pm 2\%$.

is[5] 3.3%. If we seek the reason for the possible discrepancy in the theory, we would estimate that the crudest of the approximations which we used is ignoring the presence of the rear face of the plate (the model of a half-plane) in calculating the effect of the concentrated forces[6] **pp**.

CONCLUSION

Let us summarize the progress which has been made in this study.

1. We have demonstrated that it is possible to select samples of α-quartz (the only material of which we are aware which is available as a high-quality single crystal and whose point group lacks a center of symmetry) which are of quality high enough to allow the observation of a pendulum pattern during thermal-neutron diffraction. This is true even when the elastic deformation of the single crystal is small. This circumstance raises the possibility of a future experimental study of the interaction of a neutron with strong electric fields (up to $3 \cdot 10^8$).

2. We have shown that the dynamic theory of diffraction by slightly deformed single crystals, in its present form, can also be applied directly to the case in which external forces (more specifically, a gravitational force) are applied to a particle being diffracted.

We have pointed out that a deformation (bending) of a crystal will, by changing the symmetry of the problem, make it possible in principle to see effects which do not occur in a planar (undeformed) crystal.

3. We have experimentally observed and theoretically described a new effect: an effect of the force of gravity on the diffraction of thermal neutrons in an elastically curved single crystal.

We wish to thank K. E. Kir'yanov for stimulating discussions and consultations; A. Z. Andreev, A. P. Bulkin, V. Ya. Kezerashvili, B. P. Kharchenkov, and A. F. Shchebetov for developing and fabricating the in-channel neutron duct; A. I. Kurbakov and V. A. Trunov for studying the quality of the crystals on the γ diffractometer; V. A. Priemyshev and N. I. Timoshuk for consultation and for fabricating the high-precision bending apparatus; N. V. Polunin, L. E. Samsonov, and S. I. Khakhalin for developing and adjusting the electronics; Yu. P. Platonova, V. V. Skorobogatov, and A. N. Litvinenko for assistance in producing and processing the optical interferograms during the measurement of the radii of curvature of the crystal; V. I. Gavreshev for participation in the measurements; and the staff at the VVR-M reactor of the Leningrad Institute of Nuclear Physics.

[1)]Since the deformations, the effective forces, and the "velocities" are small [$(dz/cdy)^2 \ll 1$], we are using the nonrelativistic version of the equation of motion, (4).

[2)]The forces $\mathbf{p}'\mathbf{p}'$ have also been taken into account by replacing $2a = 21.5$ mm with $2a = 80$ mm and $L - y \to y$ in (14). Their contribution increases $\bar{\beta}$ by $\approx 7\%$. The effect of $\mathbf{p}'\mathbf{p}'$ on f_{p2} and the reference surface can be ignored.

[3)]The polarization of the neutrons is unimportant in this experiment. We tested this point by recording certain points with a filter in the beam which definitely depolarized the neutrons.

[4)]In the region in which the gravitational effect is approximately constant in Fig. 4 we carried out a control experiment, in which we rotated the crystal with the bending apparatus 180° around the y axis (Fig. 1). The gravitational effect—the difference between the contrast values in the upper and lower positions of the instrument—measured by the standard procedure, changed sign after this rotation, as expected.

[5)]We carried out calculations on the trivial gravitational effect due to mechanical deformations from the change in the direction of the force of gravity during the rotation of the instrument. We estimate this trivial effect to be $\approx 1/25$ of the effect of interest here (i.e., insignificant).

[6)]The replacement of $\beta(y)$ by $\bar{\beta}$ [relation (18)] is of minor importance. Our numerical calculations showed that the particular functional dependence $\beta(y)$ has essentially no effect on the results, provided that $\bar{\beta}$ is kept the same.

[1]B. W. Batterman and H. Cole, Rev. Mod. Phys. **36**, 681 (1964).
[2]M. Forte, Phys. J. G. **9**, 745 (1983).
[3]N. Kato, J. Phys. Soc. Jpn. **18**, 1785 (1963); **19**, 67, 971 (1964).
[4]O. I. Sumbaev, Preprint LIYaF-676, Leningrad Institute of Nuclear Physics, 1981.
[5]S. A. Werner, Phys. Rev. **B21**, 1774 (1980).
[6]Z. G. Pinsker, *Rentgenovskaya kristalloptika (Crystal X-Ray Optics)*, Nauka, Moscow, 1982, p. 308.
[7]S. G. Lekhnitskiĭ, *Teoriya uprugosti anizotropnogo tela*, Nauka, Moscow, 1977 (Theory of Elasticity of an Anisotropic Body, Mir, Moscow, 1981).
[8]D. Malacara, *Optical Shop Testing*, Wiley-Interscience, New York, 1978.
[9]O. I. Sumbaev, *Kristall-difraktsionnye gamma-spektrometry (Crystal-Diffraction γ Spectrometers)*, Atomizdat, Moscow, 1963.
[10]V. L. Alekseev, A. I. Kurbakov, and V. A. Trunov, Preprint LIYaF-1345, Leningrad Institute of Nuclear Physics, 1987.

Translated by Dave Parsons